

Thermodynamic analysis of absorption refrigeration system based on entropy generation

Omer Kaynakli* and Recep Yamankaradeniz

Department of Mechanical Engineering, Faculty of Engineering and Architecture, Uludag University, TR-16059, Bursa, Turkey

In this study, the first and second law thermodynamic analysis of a single-stage absorption refrigeration cycle with water/lithium bromide as working fluid pair is performed. Thermodynamic properties of each point in the cycle are calculated using related equations of state. Heat transfer rate of each component in the cycle and some performance parameters are calculated from the first law analysis. From the second law analysis, the entropy generation of each component (\dot{S}_j) and the total entropy generation of all the system components (\dot{S}_t) are obtained. Variation of the performance and entropy generation of the system are examined at various operating conditions. The results show that high coefficient of performance (COP) value is obtained at high generator and evaporator temperatures, and also at low condenser and absorber temperatures. With increasing generator temperature, total entropy generation of the system decreases. Whereas maximum entropy generation occurs in the generator at various operating conditions, entropy generation in the refrigerant heat exchanger, expansion valve and solution pump is negligibly small.

Keywords: Absorption refrigeration, coefficient of performance, entropy generation, thermodynamic analysis.

In recent years, theoretical and experimental researches on the absorption refrigeration system (ARS) have increased, because these systems harness inexpensive energy sources (like waste heat from gas and steam turbines, solar, geothermal, biomass) in comparison to vapour compression systems¹. Besides, ARSs cause no ecological dangers, such as depletion of ozone layer and global warming, and hence they are environment-friendly. In order to protect the ozone layer, CFC-free conventional compression systems are currently being developed², mainly with HFCs. Nevertheless, these new refrigerants produce some greenhouse effect and might be banned in the next decades³. As already known, ARSs using water–lithium bromide working fluid pair are used extensively in air-conditioning and other high-temperature applications. However, with water as the refrigerant, they are not suitable for use in any applications where the evaporator is below 0°C.

A suitable working fluid is one of the most important factors affecting the performance of the ARSs. Hence many researchers have focused on investigating new working fluid pairs to improve the performance of the ARSs^{4–8}. Water-based vapour-absorption refrigeration system with four binary mixtures has been used in the study by Saravanan and Maiya⁴. Sun⁵ has provided thermodynamic properties of ammonia-based binary mixtures (NH₃–H₂O, NH₃–LiO₂, NH₃–NaSCN) and the performances of the cycles were compared using the first law of thermodynamics.

The basis of thermodynamics is stated in the first and second laws. The first law of thermodynamic analysis is still the most commonly used method in the analysis of thermal systems. The first law is concerned only with the conservation of energy, and it gives no information on how, where, and how much the system performance is degraded. The second law of thermodynamic analysis is a powerful tool in the design, optimization, and performance evaluation of energy systems⁹.

The continuous increase in the cost and demand for energy has led to more research and development to utilize available energy resources efficiently by minimizing waste energy. The principles of the second law of thermodynamics are effective to identify the components for high entropy generation and for minimizing the total entropy generation for improved performance of thermal systems. In order to increase the efficiency of a system, the entropy generation should be minimized. Information about ‘which component of the absorption refrigeration system should be developed’ can be given by the second law analysis^{10–13}.

The second law analysis calculates the system performance based on entropy generation, which always increases owing to thermodynamic irreversibility. Some researchers^{13,14} have used the principle of entropy generation minimization to analyse different systems to improve the performance, while others^{10,15} have used the exergy analysis based on the second law. Wall¹⁶ has presented a number of exergy-based concepts and methods, e.g. efficiency concepts, exergy flow diagrams, exergy utility diagrams, life cycle exergy analysis and exergy economy optimization. Ishida and Ji¹⁷ have used the graphical exergy methodology based on energy-utilization diagrams for the analysis of absorption heat transformer. Cornelissen

*For correspondence. (e-mail: kaynakli@uludag.edu.tr)

and Hirs¹⁸ have used the life cycle method for a heat exchanger. Furthermore, an availability analysis has been carried out for each component in the ARS using water/lithium bromide and ammonia/water pairs by Karakas *et al.*¹⁹. In order to improve present understanding of the second law-based methods and their applications to the various thermal systems, further investigations are needed. In addition to these realities, Dincer²⁰ emphasizes that analyses based on the second law would play an important role in solving some environmental problems.

ARSs which consider the coefficient of performance (COP) of systems based only on energy analysis without considering entropy generation in various components of the systems have been discussed^{21–23}. Srihirin *et al.*²⁴ presents a literature review on absorption refrigeration technology such as various types of ARSs, research on working fluids, and improvement of absorption processes. Joudi and Lafta²⁵ developed a steady-state computer simulation model to predict the performance of an ARS using LiBr/H₂O as a working pair. Detailed first law-based thermodynamic performance analyses of LiBr/H₂O and NH₃/H₂O single stage ARSs are discussed by Kaynakli and Yaman-karadeniz²⁶. However, all of above-mentioned studies are based only on energy and mass balance equations.

In recent years, there has been a growing interest in the use of the principles of the second law of thermodynamics for analysing and evaluating the thermodynamic performance of thermal systems as well as their technologies. Adopting this approach, in this study the first and second law of thermodynamic analysis of single-stage absorption refrigeration cycle with water/lithium bromide as working fluid pair is performed. Thermodynamic properties of each point (the inlet and outlet of each component) in the cycle are calculated using related equations of state. Heat transfer rate of each component in the cycle and some performance parameters (circulation ratio f , COP) are calculated from the first law analysis. From the second law analysis, the entropy generation of each component and the total entropy generation of all the system components are obtained. Variation of the performance and entropy generation of the system are examined at various operating conditions. Simulation results are presented in tabular and graphical form.

System description and mathematical model

A typical water–lithium bromide absorption refrigeration system is illustrated in Figure 1. The system includes a generator, absorber, condenser, evaporator, pump, expansion valves, solution heat exchanger (SHE) and refrigerant heat exchanger (RHE, precooler).

Mass balance equations of the solution and lithium bromide at the generator can be written as follows:

$$\dot{m}_{\text{WS}} = \dot{m}_{\text{SS}} + \dot{m}_{\text{R}}, \quad (1)$$

$$\dot{m}_{\text{WS}} X_{\text{WS}} = \dot{m}_{\text{SS}} X_{\text{SS}}, \quad (2)$$

where \dot{m} is the mass flow rate (kg s⁻¹), X the lithium bromide concentration, WS, weak solution, SS, strong solution and R, refrigerant.

The circulation ratio (f) can be defined as the ratio of the mass flow rate of the solution through the pump to the mass flow rate of the working fluid. It must be noted that f represents the required pumping energy. It can be expressed in terms of concentrations as follows:

$$f = \frac{\dot{m}_{\text{WS}}}{\dot{m}_{\text{R}}} = \frac{X_{\text{SS}}}{X_{\text{SS}} - X_{\text{WS}}}. \quad (3)$$

The measure of performance of refrigerators is expressed in terms of COP, defined as:

$$\text{COP} = \frac{\dot{Q}_{\text{E}}}{\dot{Q}_{\text{G}} + \dot{W}_{\text{P}}}, \quad (4)$$

where \dot{Q} is the heat transfer rate (kW), \dot{W} the pump power (kW), E the evaporator, G the generator and P the Pump.

Mass flow rate of circulated refrigerant can be calculated as follows:

$$\dot{m}_{\text{R}} = \frac{\dot{Q}_{\text{E}}}{q_{\text{E}}}. \quad (5)$$

The equations for the first law of thermodynamics (energy balance) for components of the ARS are expressed as follows:

$$\dot{Q}_{\text{A}} = \dot{m}_{\text{R}} [h_6 + (f-1)h_{12} - fh_7] = \dot{m}_{\text{a}} (h_{18} - h_{17}), \quad (6)$$

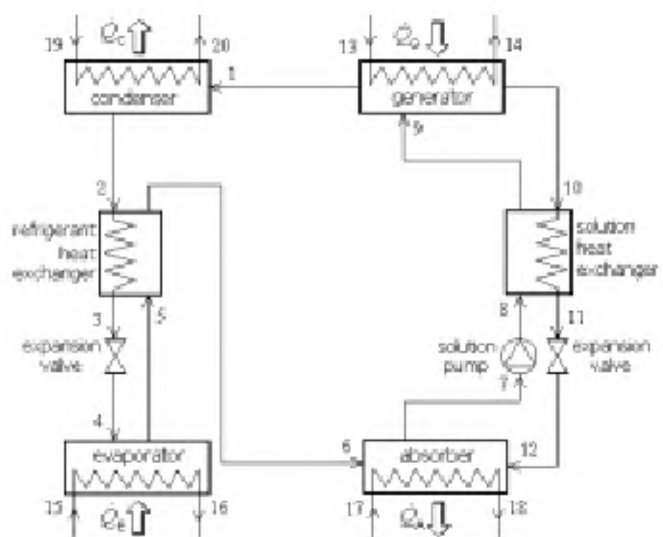


Figure 1. Schematic diagram of the water–lithium bromide ARS.

$$\dot{Q}_C = \dot{m}_R (h_1 - h_2) = \dot{m}_a (h_{20} - h_{19}), \quad (7)$$

$$\dot{Q}_G = \dot{m}_R [h_1 + (f-1)h_{10} - fh_9] = \dot{m}_{wv} (h_{13} - h_{14}), \quad (8)$$

$$\dot{Q}_E = \dot{m}_R (h_5 - h_4) = \dot{m}_a (h_{15} - h_{16}), \quad (9)$$

$$\dot{Q}_{SHE} = \dot{m}_R (f-1)(h_{10} - h_{11}) = \dot{m}_R f (h_9 - h_8), \quad (10)$$

$$\dot{Q}_{RHE} = \dot{m}_R (h_2 - h_3) = \dot{m}_R (h_6 - h_5), \quad (11)$$

$$\dot{W}_P = \dot{m}_R f (h_8 - h_7) = \dot{m}_R f v_R (p_C - p_E) / \eta_P, \quad (12)$$

where h is the specific enthalpy (kJ kg^{-1}), v the specific volume ($\text{m}^3 \text{kg}^{-1}$), p the pressure, h the efficiency, A the absorber, a the air, C the condenser and WV the water vapour.

The second law of thermodynamics is sometimes called the law of entropy as it introduces the important property called entropy. Entropy can be thought of as a measure of how close a system is to equilibrium; it can also be thought of as a measure of the disorder in the system. The second law defines the direction in which a specific thermal process can take place, and is sometimes given as a statement that precludes perpetual-motion machines of the second kind.

It is important to understand the meaning of reversible. All natural and artificial processes are irreversible, i.e. generate entropy by friction, heat flow or mass flow. Unlike energy, entropy is not conserved; analysis of the second law provides information as to where the real inefficiencies in a system lie. Entropy generation is associated with thermodynamic irreversibility, which is common in all types of heat-transfer processes.

The equations for the second law of thermodynamics (entropy generation) for each component of the ARS are expressed as follows:

$$\dot{S}_A = \dot{m}_R [fs_7 - s_6 - (f-1)s_{12}] + \dot{m}_a (s_{18} - s_{17}), \quad (13)$$

$$\dot{S}_C = \dot{m}_R (s_2 - s_1) + \dot{m}_a (s_{20} - s_{19}), \quad (14)$$

$$\dot{S}_G = \dot{m}_R [s_1 + (f-1)s_{10} - fs_9] + \dot{m}_{wv} (s_{14} - s_{13}), \quad (15)$$

$$\dot{S}_E = \dot{m}_R (s_5 - s_4) + \dot{m}_a (s_{16} - s_{15}), \quad (16)$$

$$\dot{S}_{SHE} = \dot{m}_R (f-1)(s_{11} - s_{10}) + \dot{m}_R f (s_9 - s_8), \quad (17)$$

$$\dot{S}_{RHE} = \dot{m}_R (s_3 - s_2) + \dot{m}_R (s_6 - s_5), \quad (18)$$

$$\dot{S}_P = \dot{m}_R f (s_8 - s_7), \quad (19)$$

$$\dot{S}_{SEV} = \dot{m}_R (f-1)(s_{12} - s_{11}), \quad (20)$$

$$\dot{S}_{REV} = \dot{m}_R (s_4 - s_3), \quad (21)$$

where \dot{S} is the entropy generation rate (kW K^{-1}), s the specific entropy ($\text{kJ kg}^{-1} \text{K}^{-1}$), SEV the solution expansion value and REV the refrigerant expansion value.

The total entropy generation of the absorption refrigeration cycle is the sum of entropy generation in each component, therefore:

$$\begin{aligned} \dot{S}_t = \sum_{j=1}^N \dot{S}_j = \dot{S}_A + \dot{S}_C + \dot{S}_G + \dot{S}_E + \dot{S}_{SHE} \\ + \dot{S}_{RHE} + \dot{S}_P + \dot{S}_{SEV} + \dot{S}_{REV}, \end{aligned} \quad (22)$$

where N is the total number of components in the ARS.

To simplify the modelling of the system, several assumptions were made: (i) The system operates in a steady state. (ii) Pressure drop along the fluid flow is negligible. (iii) In the condenser, the refrigerant condenses to a saturated liquid, while in the evaporator the refrigerant evaporates to a saturated vapour.

In the analyses, the properties of water/steam are obtained from correlations provided by ASHRAE²⁷. The properties of lithium bromide solution, except for density and entropy, are obtained from correlations found in Talbi and Agnew¹⁵, and Mostafavi and Agnew²⁸. The density and entropy of the $\text{H}_2\text{O}/\text{LiBr}$ solution is obtained from Kaita²⁹ and Chua *et al.*³⁰ respectively.

Results and discussion

Tables 1 and 2 show the simulation results for the thermodynamic properties and heat transfer rates of each component respectively. In this simulation, calculations were performed for 10 kW cooling load and the parameters were taken as $T_E = 4^\circ\text{C}$, $T_C = 38^\circ\text{C}$, $T_A = T_C + 2^\circ\text{C}$, $T_G = 90^\circ\text{C}$, $\varepsilon_{SHE} = \varepsilon_{RHE} = 0.50$ (ε is effectiveness) and $\eta_P = 0.90$. In Table 1, chemical composition and mass flow rates are provided along with temperature, concentration, enthalpy and entropy values of the working fluids. As seen from Table 2, compared to other components the generator heat transfer rate is the highest and the solution pump power is the lowest. Thus the effect of the pump on the total energy inputs is negligible. Moreover, the heat transfer rate of the refrigerant heat exchanger is lower than that of the solution heat exchanger due to mass flow rate and temperature difference between the fluids. Some performance parameters (f and COP) are also presented in Table 2.

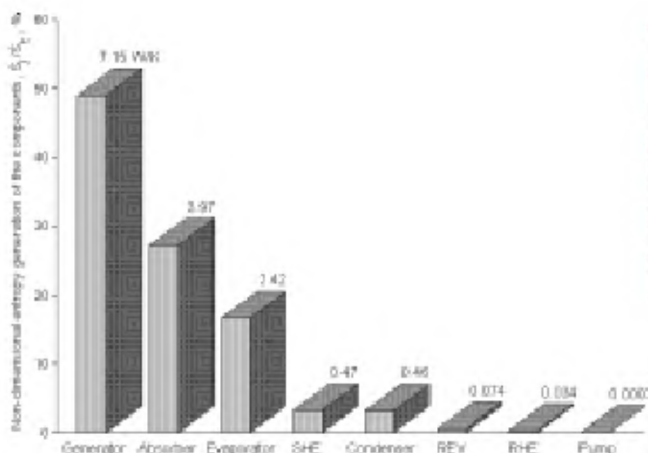
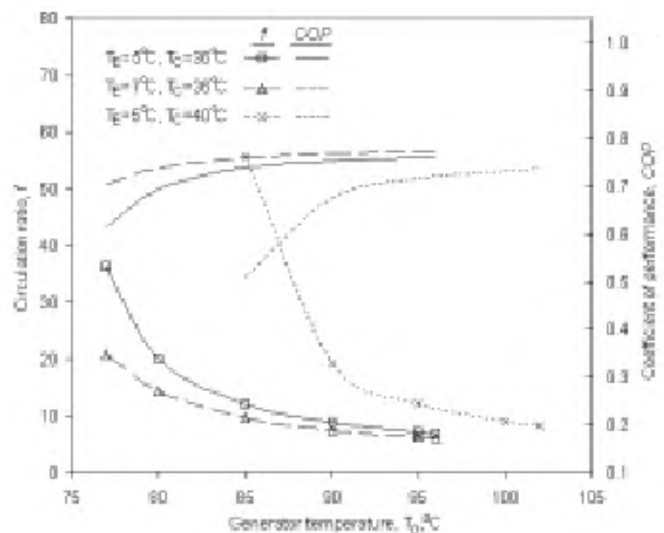
The ratio of the entropy generation in each component (\dot{S}_j) to the total entropy generation of the system (\dot{S}_t) is defined as the non-dimensional entropy generation. Figure 2 shows the non-dimensional entropy generation and entropy generation rates of each component at the same working conditions in Tables 1 and 2. The generator has the

Table 1. Thermodynamic properties of each state point

State point	Chemical composition	T (°C)	X (%)	\dot{m} (kg/s)	h (kJ/kg)	s (kJ/kg K)
1	Water vapour	90.00	0.00	0.0042	2663.15	8.31151
2	Water	38.00	0.00	0.0042	159.22	0.54414
3	Water	30.32	0.00	0.0042	127.06	0.37400
4	Water	4.00	0.00	0.0042	127.06	0.45772
5	Water vapour	4.00	0.00	0.0042	2506.73	9.05024
6	Water vapour	21.00	0.00	0.0042	2538.88	8.21773
7	Water/LiBr	40.00	58.43	0.0569	107.81	0.23729
8	Water/LiBr	40.00	58.43	0.0569	107.81	0.23730
9	Water/LiBr	61.61	58.43	0.0569	150.49	0.36649
10	Water/LiBr	90.00	63.09	0.0527	225.90	0.48731
11	Water/LiBr	65.00	63.09	0.0527	179.82	0.35680
12	Water/LiBr	65.00	63.09	0.0527	179.82	0.35680
13	Air	25.00	—	1.0	0.00	0.00000
14	Air	35.35	—	1.0	10.52	0.03426
15	Air	25.00	—	1.0	0.00	0.00000
16	Air	38.79	—	1.0	14.01	0.04536
17	Water vapour	200.00	—	0.1	2878.50	8.82352
18	Water vapour	126.00	—	0.1	2733.18	8.49072
19	Air	25.00	—	1.0	0.00	0.00000
20	Air	15.16	—	1.0	-10.00	-0.03368

Table 2. Heat transfer rates of components and performance parameters of the system

Component	Heat transfer rate (kW)
Absorber (\dot{Q}_A)	14.009
Condenser (\dot{Q}_C)	10.522
Generator (\dot{Q}_G)	14.531
Evaporator (\dot{Q}_E)	10.000
Pump (\dot{W}_p)	0.052
Solution heat exchanger (\dot{Q}_{SHE})	2.428
Refrigerant heat exchanger (\dot{Q}_{RHE})	0.135
Performance parameters of the ARS	
Circulation ratio (f)	13.54
Coefficient of performance (COP)	0.69

**Figure 2.** Non-dimensional entropy generation of each component in the ARS.**Figure 3.** Variation of f and COP with generator temperature at different condenser and evaporator temperatures ($T_A = T_C + 2^\circ\text{C}$; $\epsilon_{SHE} = \epsilon_{RHE} = 0.60$; $\eta_P = 0.90$).

highest entropy generation with the 49.0% (7.15 W/K); the next highest entropy generation occurred in the absorber with the 27.2% (3.97 W/K). Since entropy generation rates in the pump, expansion valves and refrigerant heat exchanger are small, their effects on the total entropy generation are negligible. Under the same working conditions, the total energy dissipation (the total entropy generation rate) of single-stage ARS is 14.6 W/K.

Figure 3 shows variation f and COP with generator temperature at different condenser and evaporator temperatures. By decreasing the condenser temperature and

increasing the evaporator temperature, performance of the system increases. While the f value decreases with increasing generator temperatures, COP value increases. In general, to obtain high COP values it is necessary to operate the cycle at low values of f , which implies high values of T_G and T_E and low values of T_C and T_A .

Figure 4 shows variation of both the entropy generation rate and non-dimensional entropy generation of the absorber as a function of generator temperature. Entropy generation rate of the absorber approximately remains constant with generator temperatures at different evaporator temperatures (~ 3.5 W/K at $T_E = 5^\circ\text{C}$, ~ 3.3 W/K at $T_E = 7^\circ\text{C}$). Variation of the condenser temperature has greater effect than that of the evaporator temperature on entropy generation in the absorber. As the condenser temperature increases, both the entropy generation rate and non-dimensional entropy generation of the absorber increase. Because 25–30% of the total entropy generation in the system takes place in the absorber, it is one of the most important components of the ARS, like the generator.

Figure 5 shows variation of both the entropy generation rate and non-dimensional entropy generation of the condenser with generator temperature. The entropy generation rate and non-dimensional entropy generation of the condenser increase with an increase in generator temperature. While variation of the evaporator temperature does not affect the entropy generation of the condenser, both the entropy generation rate and non-dimensional entropy generation of the condenser increase with increasing condenser and generator temperatures.

Variation of the entropy generation rate and non-dimensional entropy generation of the generator with the generator temperature at different evaporator and condenser temperatures is shown in Figure 6. The entropy generation in the generator slightly decreases with the

generator temperature. The non-dimensional entropy generation of the generator decreases as the condenser temperature increases and the evaporator temperature decreases. On the other hand, entropy generation of the generator is an important fraction of the total entropy generation in the system basically due to the temperature difference between the heat source and the working fluid. Therefore, in order to decrease the total entropy generation of the system, the generator should be regarded as a system component which should be developed.

Figure 7 shows variation of the entropy generation rate and non-dimensional entropy generation of the evaporator with generator temperature. The entropy generation in the

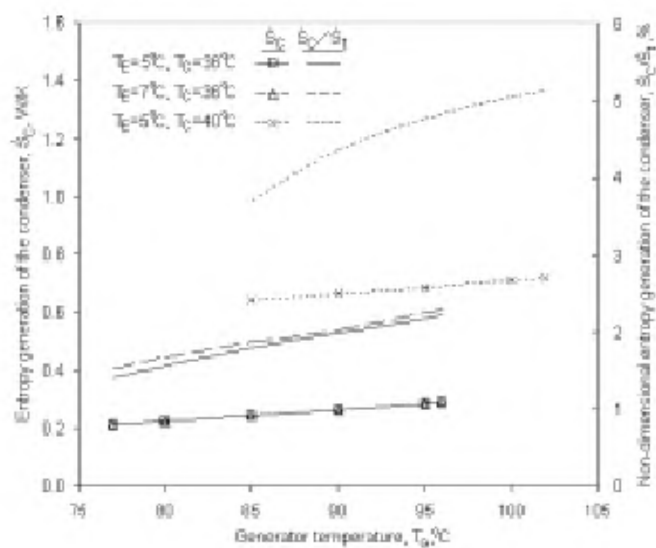


Figure 5. Variation of entropy generation rate and non-dimensional entropy generation of the condenser with generator temperature ($T_A = T_C + 2^\circ\text{C}$; $\varepsilon_{\text{SHE}} = \varepsilon_{\text{RHE}} = 0.60$; $\eta_p = 0.90$).

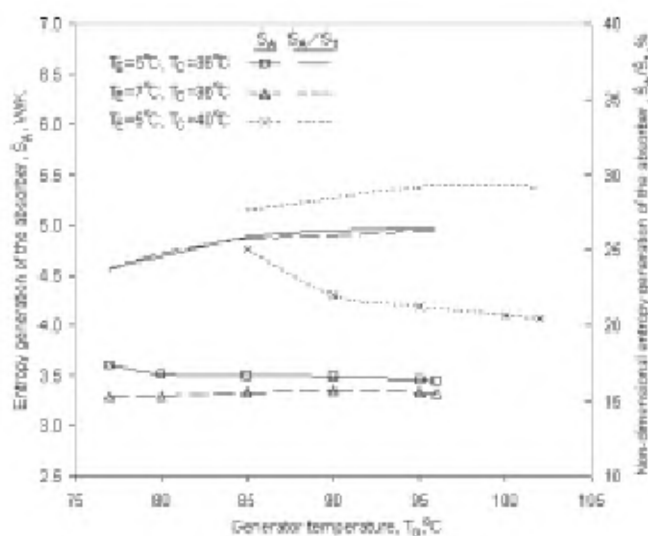


Figure 4. Variation of entropy generation rate and non-dimensional entropy generation of the absorber with generator temperature ($T_A = T_C + 2^\circ\text{C}$; $\varepsilon_{\text{SHE}} = \varepsilon_{\text{RHE}} = 0.60$; $\eta_p = 0.90$).

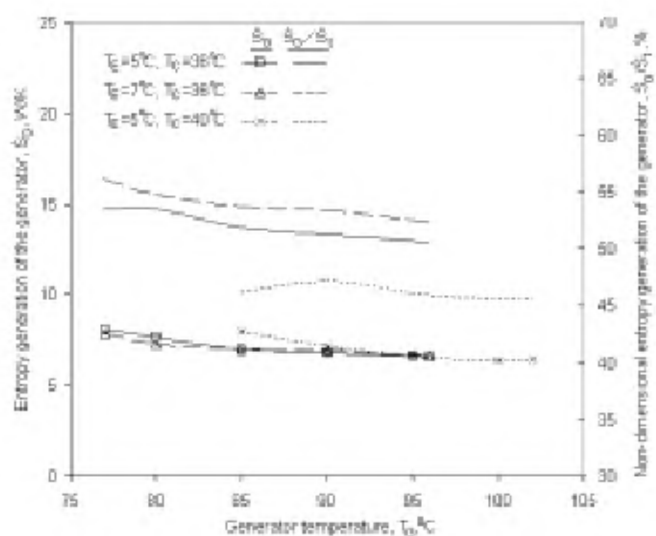


Figure 6. Variation of entropy generation rate and non-dimensional entropy generation of the generator with generator temperature ($T_A = T_C + 2^\circ\text{C}$; $\varepsilon_{\text{SHE}} = \varepsilon_{\text{RHE}} = 0.60$; $\eta_p = 0.90$).

evaporator does not change with the condenser and generator temperatures. However, as the evaporator temperature increases, entropy generation of the evaporator decreases. The non-dimensional entropy generation of the evaporator decreases with increasing evaporator and condenser temperatures, and increases with increasing generator temperature.

Figures 8 and 9 show variation of the entropy generation rate and non-dimensional entropy generation of SHE and RHE as a function of generator temperature. For SHE, entropy generation increases with increasing condenser temperature and decreasing evaporator temperature. For RHE, entropy generation increases with increasing con-

denser and evaporator temperatures, but it does not change with variation of the generator temperature. The condenser temperature has greater effect on entropy generation in comparison to the evaporator temperature for both components. Due to the fact that the ratio of the entropy generation in RHE to the total entropy generation of the system is even lower than 1%, its effect on the total entropy generation of the system is negligible.

Variations of entropy generation rate and non-dimensional entropy generation of the solution pump and refrigerant expansion value (REV) with the generator temperature are shown in Figures 10 and 11. It can be seen from Figure 10 that both the entropy generation rate and non-dimensional

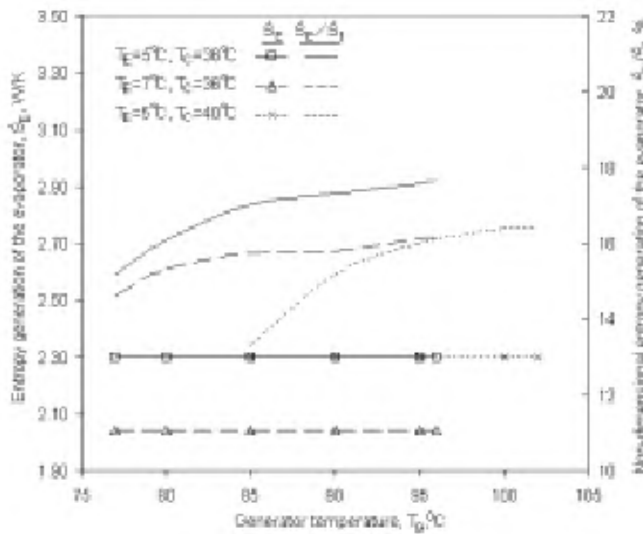


Figure 7. Variation of entropy generation rate and non-dimensional entropy generation of the evaporator with generator temperature ($T_A = T_C + 2^\circ\text{C}$; $\epsilon_{\text{SHE}} = \epsilon_{\text{RHE}} = 0.60$; $\eta_P = 0.90$).

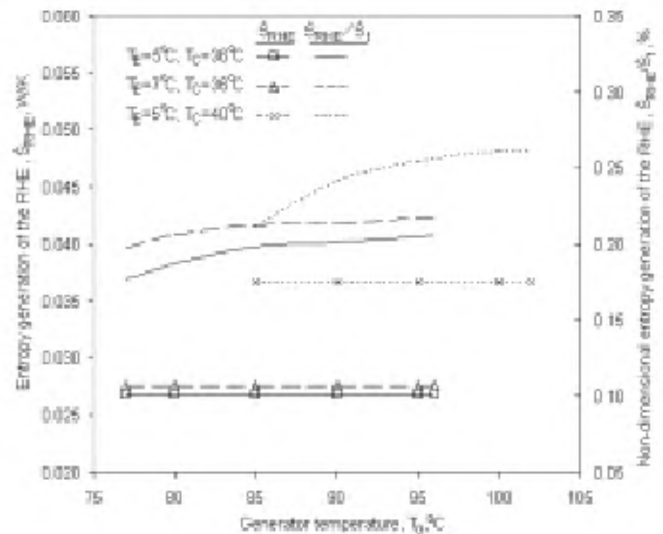


Figure 9. Variation of entropy generation rate and non-dimensional entropy generation of RHE with generator temperature ($T_A = T_C + 2^\circ\text{C}$; $\epsilon_{\text{SHE}} = \epsilon_{\text{RHE}} = 0.60$; $\eta_P = 0.90$).

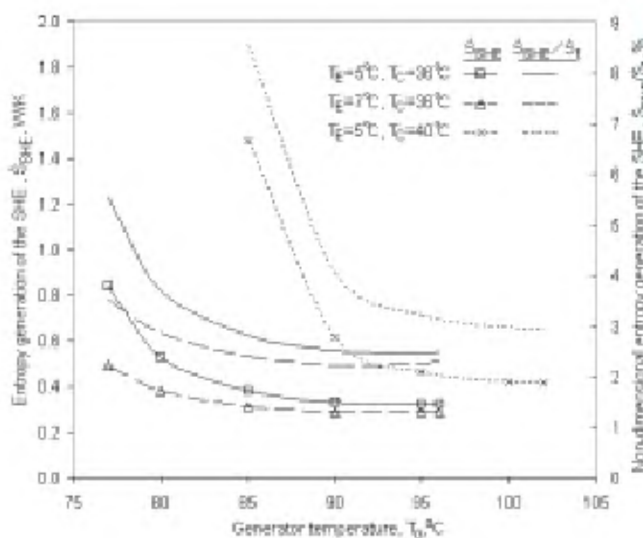


Figure 8. Variation of entropy generation rate and non-dimensional entropy generation of SHE with generator temperature ($T_A = T_C + 2^\circ\text{C}$; $\epsilon_{\text{SHE}} = \epsilon_{\text{RHE}} = 0.60$; $\eta_P = 0.90$).

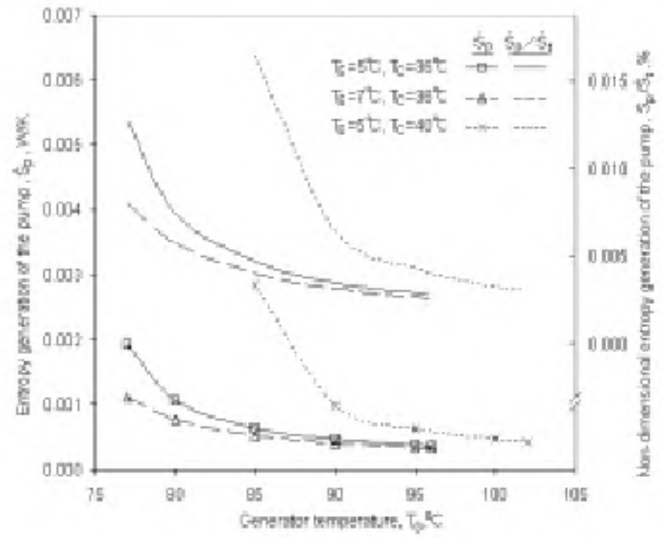


Figure 10. Variation of entropy generation rate and non-dimensional entropy generation of the pump with generator temperature ($T_A = T_C + 2^\circ\text{C}$; $\epsilon_{\text{SHE}} = \epsilon_{\text{RHE}} = 0.60$; $\eta_P = 0.90$).

entropy generation of the solution pump decrease when the generator temperature increases. On the contrary, non-dimensional entropy generation of REV increases with increase in the generator temperature (Figure 11). Furthermore, while entropy generation of the REV does not change with the generator temperature, it decreases with an increase in the evaporator temperature and increases with an increase in the condenser temperature. Moreover, Figures 10 and 11 also show that the non-dimensional entropy generation of the pump and REV is a small fraction of the total entropy generation in the system; hence their effects on entropy generation are negligible. Under the examined conditions, the ratio of entropy generation in the pump to

the total entropy generation of the system varies from 0.002 to 0.015% and that in REV varies from 0.3 to 0.5%.

Variation of the sum of the entropy generation rate in each component (the total entropy generation rate of the system) with the generator temperature is shown in Figure 12. As the generator temperature increases, total entropy generation rate of the system decreases. The decrease in the total entropy generation rate at low generator temperatures is stronger than that at higher generator temperatures. Figure 12 also shows that total entropy generation rate of the system has high values at low evaporator and high condenser temperatures. But the effect of the condenser temperature is greater than that of the evaporator temperature on the total entropy generation rate of the system. In this respect, operating conditions of the condenser are more important than those of the evaporator. As mentioned earlier, the generator plays the biggest part in the total entropy generation rate of the system. In Figure 12, at $T_E = 5^\circ\text{C}$, $T_C = 40^\circ\text{C}$ and $T_G = 85^\circ\text{C}$, the total entropy generation rate of the system is 17.3 W/K. About 46% of this total entropy generation is produced by the generator. Similar situation is seen at other operating conditions; thus the generator is the most important in the system.

Conclusion

The present study applies the second law of thermodynamics using the constituted mathematical model to study the performance of lithium bromide/water ARS, when some design parameters are varied. The computational model based on entropy generation is presented to investigate the effects of the evaporator, condenser and generator temperatures on the entropy generation of individual components, total entropy generation of the system, the COP and f values of the absorption refrigeration cycle. Solution procedure and application steps are clearly presented and results are comprehensively discussed. Some concrete results are obtained to provide better understanding of the performance improvement techniques of common thermal systems.

Using the developed computer simulation, after calculating the thermodynamic properties (T , X , \dot{m} , h , s) of each state point of the cycle, heat transfer rates of components, pump work rate and performance parameters of the system are calculated. Then, variation of entropy generation and non-dimensional entropy generation in each component is investigated under different operating conditions. It is found that as expected, with a decrease in the condenser-absorber temperatures, and increase in the generator-evaporator temperatures, the performance of the system increases. Besides, while the f value decreases with increasing generator temperatures, COP value increases. The results also show that entropy generation in the refrigerant expansion valve, refrigerant heat exchanger and solution pump are small fractions of the total entropy generation in the ARS.

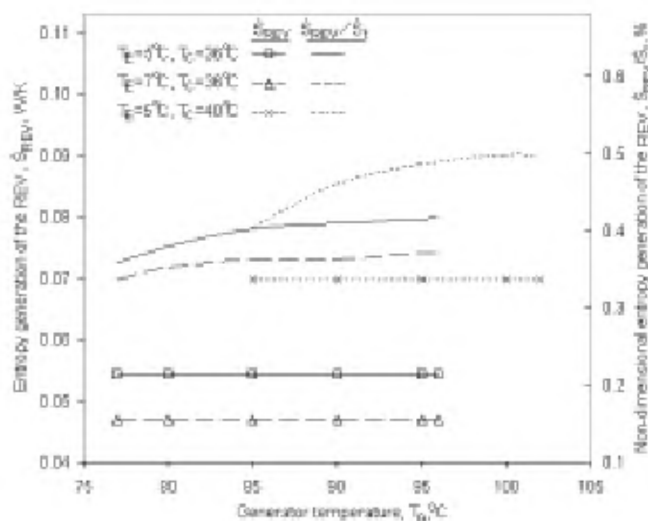


Figure 11. Variation of entropy generation rate and non-dimensional entropy generation of REV with generator temperature ($T_A = T_C + 2^\circ\text{C}$; $\epsilon_{\text{SHE}} = \epsilon_{\text{RHE}} = 0.60$; $\eta_P = 0.90$).

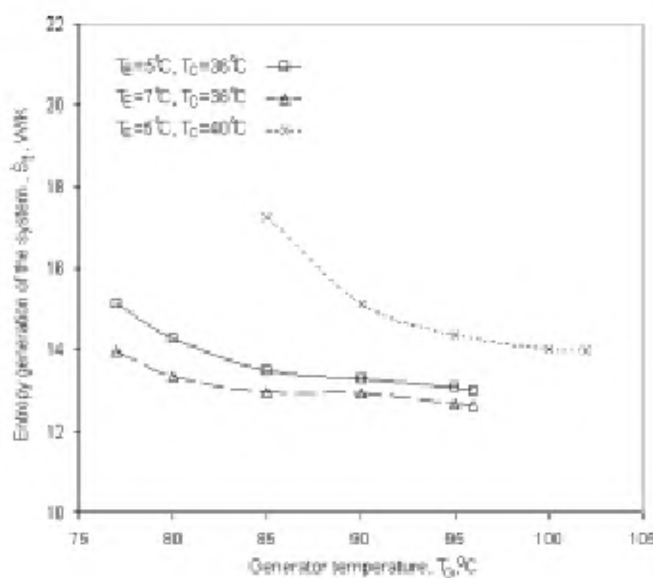


Figure 12. Variation of total entropy generation rate of the system with generator temperature ($T_A = T_C + 2^\circ\text{C}$; $\epsilon_{\text{SHE}} = \epsilon_{\text{RHE}} = 0.60$; $\eta_P = 0.90$).

The non-dimensional entropy generation in the generator, absorber and evaporator is high compared to other components in the cycle. Since the sum of the non-dimensional entropy generation of these components is approximately 90%, they are considered the most important components of the ARS. These components should be developed to provide less entropy generation. Especially, the generator has greater effect on the COP and entropy generation in the system. Thus it can be clearly stated that the generator is the most important component of the ARS.

Finally, the second law of thermodynamic analysis based on entropy generation is obviously a useful tool in engineering design and optimization, particularly of power and energy systems. This analysis offers an excellent complement to other tools and is recommended for further application.

1. Aphornratana, S. and Eames, I. W., Thermodynamic analysis of absorption refrigeration cycles using the second law of thermodynamics method. *Int. J. Refrig.*, 1995, **18**, 244–252.
2. Hewitt, N. J. and McMullan, J. T., The replacement of CFCs in refrigeration equipment by environmentally benign alternatives. *Appl. Therm. Eng.*, 1997, **17**, 955–972.
3. Pons, M. and Kodama, A., Entropic analysis of adsorption open cycles for air conditioning. Part 1: First and second law analyses. *Int. J. Energy Res.*, 2000, **24**, 251–262.
4. Saravanan, R. and Maiya, M. P., Thermodynamic comparison of water-based working fluid combinations for a vapour absorption refrigeration system. *Appl. Therm. Eng.*, 1998, **18**, 553–568.
5. Sun, D. W., Comparison of the performance of $\text{NH}_3\text{--H}_2\text{O}$, $\text{NH}_3\text{--LiNO}_3$ and $\text{NH}_3\text{--NaSCN}$ absorption refrigeration systems. *Energy Convers.*, 1998, **39**, 357–368.
6. Arun, M. B., Maiya, M. P. and Murthy, S. S., Optimal performance of double-effect series flow vapour absorption refrigeration systems with new working fluids. *Int. J. Energy Res.*, 1998, **22**, 1001–1017.
7. Yokozeki, A., Theoretical performances of various refrigerant-absorbent pairs in a vapour-absorption refrigeration cycle by the use of equations of state. Accepted for publication in *Appl. Energy*, 2004.
8. Yoon, J. I. and Kwon, O. K., Cycle analysis of air-cooled absorption chiller using a new working solution. *Energy*, 1999, **24**, 795–809.
9. Yumrutas, R., Kunduz, M. and Kanoglu, M., Exergy analysis of vapor compression refrigeration systems. *Exergy, Int. J.*, 2002, **2**, 266–272.
10. Sozen, A., Effect of heat exchangers on performance of absorption refrigeration systems. *Energy Convers. Manage.*, 2001, **42**, 699–1716.
11. Kotas, T. J., *The Exergy Method of Thermal Plant Analysis*, Krieger Publishing Company, USA, 1995, 2nd edn.
12. Adewusi, S. A. and Zubair, S. M., Second law based thermodynamic analysis of ammonia–water absorption refrigeration systems. *Energy Convers. Manage.*, 2004, **45**, 2355–2369.
13. Bejan, A., *Advanced Engineering Thermodynamics*, John Wiley, New York, 1998.
14. Izquierdo, M., de Vega, M., Lecuona, A. and Rodriguez, P., Entropy generated and exergy destroyed in lithium bromide thermal compressors driven by the exhaust gases of an engine. *Int. J. Energy Res.*, 2000, **24**, 1123–1140.
15. Talbi, M. M. and Agnew, B., Exergy analysis: An absorption refrigerator using lithium bromide and water as the working fluids. *Appl. Therm. Eng.*, 2000, **20**, 619–630.
16. Wall, G., Exergy tools. *Proc. Inst. Mech. Eng. Part A: J. Power Energy*, 2003, **217**, 125–136.
17. Ishida, M. and Ji, J., Graphical exergy study on single stage absorption heat transformer. *Appl. Therm. Eng.*, 1999, **19**, 1191–1206.
18. Cornelissen, R. L. and Hirs, G. G., Thermodynamic optimisation of a heat exchanger. *Int. J. Heat Mass Transf.*, 1999, **42**, 951–959.
19. Karakas, A., Egrican, N. and Uygur, S., Second-law analysis of solar absorption–cooling cycles using lithium bromide/water and ammonia/water as working fluids. *Appl. Energy*, 1990, **37**, 169–187.
20. Dincer, I., Thermodynamics, exergy and environmental impact. *Energy Sources*, 2000, **22**, 723–732.
21. Romero, R. J., Rivera, W. and Best, R., Comparison of the theoretical performance of a solar air conditioning system operating with water/lithium bromide and an aqueous ternary hydroxide. *Solar Energy Mater. Solar Cells*, 2000, **63**, 387–399.
22. Sun, D. W., Computer simulation and optimization of ammonia–water absorption refrigeration systems. *Energy Sources*, 1997, **19**, 677–690.
23. Dincer, I. and Dost, S., Energy analysis of an ammonia–water absorption refrigeration system. *Energy Sources*, 1996, **18**, 727–733.
24. Srihirin, P., Aphornratana, S. and Chungpaibulpatana, S., A review of absorption refrigeration technologies. *Renew. Sustain. Energy Rev.*, 2001, **5**, 343–372.
25. Joudi, K. A. and Lafta, A. H., Simulation of a simple absorption refrigeration system. *Energy Convers. Manage.*, 2001, **42**, 1575–1605.
26. Kaynakli, O. and Yamankaradeniz, R., A comparison between $\text{H}_2\text{O--LiBr}$ and $\text{NH}_3\text{--H}_2\text{O}$ solutions in single stage absorption refrigeration system (in Turkish). *Dokuz Eylul Univ. Fen Mühendislik Dergisi*, 2003, **5**, 73–87.
27. ASHRAE, *Fundamentals Handbook*, American Society of Heating, Refrigerating and Air Conditioning Engineers, New York, 1985.
28. Mostafavi, M. and Agnew, B., The impact of ambient temperature on lithium bromide–water absorption machine performance. *Appl. Therm. Eng.*, 1996, **16**, 515–522.
29. Kaita, Y., Thermodynamic properties of lithium bromide–water solutions at high temperatures. *Int. J. Refrig.*, 2001, **24**, 374–390.
30. Chua, H. T., Toh, H. K., Malek, A., Ng, K. C. and Srinivasan, K., Improved thermodynamic property field of $\text{LiBr--H}_2\text{O}$ solution. *Int. J. Refrig.*, 2000, **23**, 412–429.

Received 1 February 2006; revised accepted 5 December 2006